

# Self-assembly of lipids in water. Exact results from a one-dimensional lattice model

Jakub Pękalski, Paweł Rogowski, and Alina Ciach\*

*Institute of Physical Chemistry, Polish Academy of Sciences, 01-224 Warszawa, Poland*

(Dated: January 26, 2022)

## Abstract

We consider a lattice model for amphiphiles in a solvent with molecules chemically similar to one part of the amphiphilic molecule. The dependence of the interaction potential on orientation of the amphiphilic molecules is taken into account explicitly. The model is solved exactly in one dimension by the transfer-matrix method. In particular, pressure as a function of concentration, correlation function and specific heat are calculated. The model is compared with the recently introduced lattice model for colloidal self-assembly, where the particles interact with the isotropic short-range attraction and long-range repulsion (SALR) potential. Similarities between the amphiphilic and the colloidal self-assembly are highlighted.

---

\*Electronic address: [aciach@ichf.edu.pl](mailto:aciach@ichf.edu.pl)

## I. INTRODUCTION

Statistical thermodynamics of simple liquids and their mixtures has been extensively studied, and thermodynamical and structural properties of such systems are well understood [1]. In particular, an accurate equation of state of the Lennard-Jones fluid has been obtained [2]. The impressive development of the theory was possible thanks to the key contributors including prof. Tomas Boublik and prof. Ivo Nezbeda. In contrast, the statistical thermodynamics of the so called soft matter systems is much less developed, and recently these systems draw increasing attention. Complex molecules, nanoparticles, colloid particles or polymers in various solvents interact with effective potentials that may have quite different forms. When the shape of the effective potential resembles the shape of interactions between atoms or simple molecules, then analogs of the gas-liquid and liquid-solid transitions occur [3]. If, however, there are competing tendencies in the interactions, then instead of the gas-liquid transition or separation of the components, a self-assembly or a microsegregation may be observed [4–9].

The competing interactions can have quite different origin and form. One important example of competing interactions is the so called short-range attraction (SA), and long-range repulsion (LR) SALR potential [10–14], consisting of a solvent-induced short-range attraction and long-range repulsion that is either of electrostatic origin, or is caused by polymeric brushes bound to the surface of the particles. The attraction favours formation of small clusters. Because of the repulsion at large distances, however, large clusters are energetically unfavourable. For increasing concentration of the particles elongated clusters and a network were observed in both experiment and theory [5, 14–17].

Competing interactions of a quite different nature are present in systems containing amphiphilic molecules such as surfactants, lipids or diblock copolymers [8, 14]. Amphiphilic molecules are composed of covalently bound polar and organic parts, and in polar solvents self-assemble into spherical or elongated micelles, or form a network in the sponge phase. In addition, various lyotropic liquid crystal phases can be stable [9, 18].

Despite of very different origin and shape of the interaction potentials, very similar patterns occur on the mesoscopic length scale in the systems interacting with the isotropic SALR potential, and in the amphiphilic solutions with strongly anisotropic interactions [14, 19]. The particles interacting with the SALR potential self-assemble into spherical or elongated

clusters or form a network, whereas the amphiphiles self-assemble into spherical or elongated micells or form the sponge phase. The distribution of the clusters or the micelles in space and the transitions between ordered phases composed of these objects are very similar.

The origin of the universal topology of the phase diagrams in the amphiphilic and SALR systems was studied in Ref.[20]. It has been shown by a systematic coarse-graining procedure that in the case of weak order the colloidal and the amphiphilic self-assembly can be described by the same Landau-Brazovskii functional [21]. The Landau-Brazovskii functional was first applied to the block-copolymers by Leibler in 1980 [22]. Later functionals of the same type were applied to microemulsions [8, 9, 23]. The Landau-Brazovskii -type functional, however, is appropriate only for weak order, where the average density and concentration are smooth, slowly varying functions on the mesoscopic length scale. Moreover, in derivation of the functional various assumptions and approximations were made. Further approximations are necessary in order to obtain solutions for the phase diagram, equation of state and correlation functions. Thus, the question of universality of the pattern formation on the mesoscopic length scale, particularly at low temperatures, is only partially solved.

We face two types of problems when we want to compare thermodynamic and structural properties in different self-assembling systems in the framework of statistical thermodynamics. First, one has to introduce generic models with irrelevant microscopic details disregarded. Second, one has to make approximations to solve the generic models, or perform simulations. It is not obvious a priori how the assumptions made in construction of the model and the approximations necessary for obtaining the solutions influence the results. In the case of simulations the simulation box should be commensurate with the characteristic size of the inhomogeneities that is to be determined. It is thus important to introduce generic models for different types of self-assembly that can be solved exactly. Exact solutions can be easily obtained in one-dimensional models, but there are no phase transitions in one dimension for temperatures  $T > 0$ . Nevertheless, the ground state (GS) can give important information about energetically favorable ordered structures, and pretransitional ordering for  $T > 0$  can be discussed based on exact results for the equation of state, correlation function and specific heat.

A generic one-dimensional lattice model for the SALR potential was introduced and solved exactly in Ref.[24]. In this model the nearest-neighbors (nn) attract each other, and the third neighbors repel each other. It is thus energetically favorable to form clusters composed of

3 particles separated by at least 3 empty sites. The GS is governed by the repulsion-to-attraction ratio  $J$  and by the chemical potential of the particles. An interesting property of the GS is strong degeneracy at the coexistence of the ordered cluster phase with the gas or liquid phases. Due to this degeneracy the entropy per site does not vanish. The collection of the microstates present for  $T = 0$  at the coexistence between the periodic and the gas or the liquid phases can be interpreted as a disordered cluster or bubble phase respectively. For  $T > 0$  pseudo phase transitions between the gas and the periodically distributed clusters, and between the periodically distributed clusters and the dense liquid phases were obtained. The equation of state (EOS) has a characteristic shape that is significantly different from the EOS in simple fluids.

A one dimensional lattice model for amphiphiles in solvents attracting one of the two parts of the amphiphilic molecule was introduced in Ref.[25]. The two models, one for the SALR and the other one for the amphiphilic system, are defined on the same level of coarse-graining, therefore by comparing the exact results we can draw conclusions on similarities of self-assembly in these systems, and the origin of these similarities. In the model introduced in Ref.[25] the GS is strongly degenerate at the phase coexistence between the pure solvent and periodically distributed bilayers, and the entropy per site does not vanish. Thus, the GS of the two models show remarkable similarity, despite quite different interaction potentials. This suggests similar origin of the formation of disordered phases with mesoscopic inhomogeneities in various systems with competing interactions.

In this work we solve exactly the model introduced in Ref.[25] by the transfer matrix method. We describe the model and its ground state in sec.2. The transfer matrix and exact expressions for the grand potential, density and correlation function are given in sec.3. In sec.4 and 5 we present our results for the EOS and the correlation function. In sec.6 we calculate the specific heat with fixed chemical potential in the grand canonical ensemble, and by using thermodynamic relations we obtain the specific heat with fixed concentration. To check our exact calculations we also perform Monte Carlo simulations and compute the specific heat with fixed concentration directly in the canonical ensemble. Our additional purpose is to verify the results of the simulations performed in a finite system by comparison with the exact results obtained in the thermodynamic limit. We cross-check the exact and the simulation results for the specific heat, because in simulations of the 2- or 3-dimensional self-assembling systems the peak in the specific heat is interpreted as a signature of a phase

transition[26]. It is thus worthwhile to compare the simulation and the exact results for this important quantity. In sec.7 our results for the mechanical, structural and thermal properties are compared with the corresponding results obtained in Ref.[24] for the SALR model.

## II. THE MODEL AND ITS GROUND STATE

### A. The model

The amphiphilic molecules consist of a hydrophilic head and a hydrophobic tail, therefore the interactions between them depend on orientations. In the case of a two-component mixture of a polar solvent and amphiphilic molecules, for example lipids, we assume that the solvent molecules attract the polar head, and effectively repel the hydrophobic tail of the amphiphilic molecule. We neglect orientational degrees of freedom of the solvent molecules. In a one-dimensional model the continuum of different orientations of amphiphiles is reduced to just two orientations (Fig.1). We assume that the molecules occupy lattice sites, and the lattice constant  $a$  is of order of the length of the amphiphilic molecule in this model. If the solvent molecules are much smaller than the amphiphilic molecules, we assume that the site is occupied by a cluster of several solvent molecules.

We assume nearest-neighbor interactions. The absolute value of the energy of two clusters of solvent molecules that occupy the nearest-neighbour sites,  $-b$ , is taken as the energy unit. We assume that the interaction between the cluster of solvent molecules and the amphiphilic molecule in the favorable (unfavorable) orientation is  $-cb$  ( $+cb$ ), and the interaction between two amphiphilic molecules in the favorable and unfavorable orientation is  $-gb$  and  $+gb$  respectively. The orientations of two amphiphilic molecules are favorable when they are oriented either head-to-head or tail-to-tail. The neighborhood of the polar head and the hydrophobic tail is unfavorable. The energies of different pairs of occupied sites are shown in Fig. 1. The model is similar to a lattice model of ternary oil-water-surfactant mixtures introduced in Ref.[27] and to a continuous model of binary mixtures with amphiphiles [28].

Different values of the parameters  $b, c, g$  may correspond to different particular mixtures. In this work we are interested in general aspects of the amphiphilic self-assembly, especially in similarities between ordering on the mesoscopic length scale in the amphiphilic and colloidal

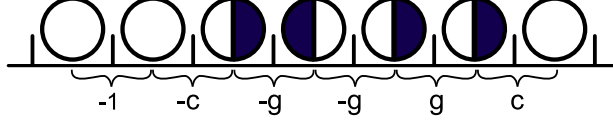


FIG. 1: The interacting pairs of occupied sites in the 1d model. The open circle represents the solvent molecule, and the light and dark semicircles represent the head and the tail of the amphiphilic molecule respectively. The unit of the inscribed energies is the absolute value of the solvent-solvent interaction energy.

systems, and in origin of these similarities. For this reason we shall not try to fit the model parameters to any particular mixture. A representative example of a system described by this model is a mixture of lipids and water. We should stress that water is a complex liquid [29–32], and micro-heterogeneities are present in aqueous solutions of polar molecules [33, 34]. However, on the mesoscopic length scale of tens or hundreds of nanometers the ordering of the water molecules plays a subdominant role.

We introduce the microscopic densities  $\hat{\rho}_i(x)$  with  $i = 1, 2, 3$  denoting the cluster of solvent molecules, and the amphiphile with the head on the left and on the right respectively.  $\hat{\rho}_i(x) = 1$  when the site  $x$  is in the state  $i$  and  $\hat{\rho}_i(x) = 0$  otherwise. Multiple occupancy of the lattice sites is excluded. We further restrict our attention to the liquid phase and assume close-packing,

$$\sum_{i=1}^3 \hat{\rho}_i(x) = 1. \quad (1)$$

Up to a state-independent constant the Hamiltonian of an open system, with the chemical-potential contribution included, can be written in the form

$$H[\{\hat{\rho}_i\}]/b = \frac{1}{2} \sum_{x=1}^L \sum_{x'=1}^L \hat{\rho}_i(x) V_{ij}(x, x') \hat{\rho}_j(x') - \sum_{x=1}^L \mu \hat{\rho}_1(x), \quad (2)$$

where the summation convention for repeated indices is used,  $L$  is the system size,  $\mu = \mu_1 - \mu_s$ ,  $\mu_1 b$  is the chemical potential of the solvent, and the chemical potential of amphiphiles,  $\mu_s b = \mu_2 b = \mu_3 b$ , is independent of orientations of the molecules. We assume periodic boundary conditions,  $L + 1 \equiv 0$ . According to the above discussion of interactions the interaction potential  $\mathbf{V}$  is

$$\mathbf{V}(x, x+1) = \begin{bmatrix} -1 & -c & c \\ c & g & -g \\ -c & -g & g \end{bmatrix} \quad (3)$$

and  $V_{ij}(x, x-1) = V_{ji}(x, x+1)$ ,  $V_{ij}(x, x+k) = 0$  for  $|k| > 1$ . In the liquid phase we can neglect density fluctuations (Eq.(1)), hence  $\hat{\rho}_1(x) = 1 - \hat{\rho}_2(x) - \hat{\rho}_3(x)$  and there are two independent densities. In a disordered phase  $\langle \hat{\rho}_i(x) \rangle = \rho_i$ , and  $\rho_1 = 1 - \rho_s$  with  $\rho_s = 2\rho_2 = 2\rho_3$  denoting the average amphiphile concentration.

## B. The ground state

At  $T = 0$  the stable structure corresponds to the global minimum of the Hamiltonian. Apart from the solvent-rich and amphiphile-rich phases we find stability of the periodic phase where amphiphilic bilayers are separated by layers of solvent. In the amphiphile-rich phase the molecules are oriented head-to-head and tail-to-tail when  $g > 0$ . In the periodic phase a solvent-occupied site is followed by 2 sites occupied by properly oriented amphiphilic molecules. The coexistence lines obtained by equating  $H/L$  in these phases are [25]

$$\mu = \begin{cases} g - 1 & \text{solvent-amphiphile} \\ \frac{2c+g-3}{2} & \text{solvent-bilayers} \\ 2(g - c) & \text{bilayers-amphiphile.} \end{cases} \quad (4)$$

The  $(c, g, \mu)$  ground state is shown in Fig. 2. The solvent-amphiphile coexistence occurs for small values of  $c$ . All the three phases coexist at the triple line  $g = 2c - 1$  and  $\mu = 2(c - 1)$ . When  $g \leq 2c - 1$  the periodic structure of solvent-separated bilayers may be present for some range of  $\mu$  and the sequence of the stable phases for increasing  $\mu$  at fixed  $c$  and  $g$  is: amphiphiles-bilayers-solvent.

At the solvent-periodic phase coexistence the separation  $l$  between the bilayers can be arbitrary, because  $H/L$  is independent of  $l$  for  $\mu$  given by Eq.(4)b [25]. Thus, the ground state is strongly degenerate and the entropy per site does not vanish. Similar degeneracy occurs at the periodic-amphiphile phase coexistence. At the periodic-amphiphile coexistence the separation between the solvent occupied sites is  $2n$  with arbitrary  $n$ , because when Eq.(4)c holds,  $H/L$  is independent of  $n$  [25].

Note that the arbitrary separation between the bilayers at the coexistence between the solvent and the periodic phase signals vanishing surface tension between the two phases. Similar degeneracy of the ground state was found earlier for the lattice model of microemulsion [35]. The very low surface tension at the coexistence between the microemulsion and the water-rich phases was attributed to the amphiphilic nature of surfactant molecules.

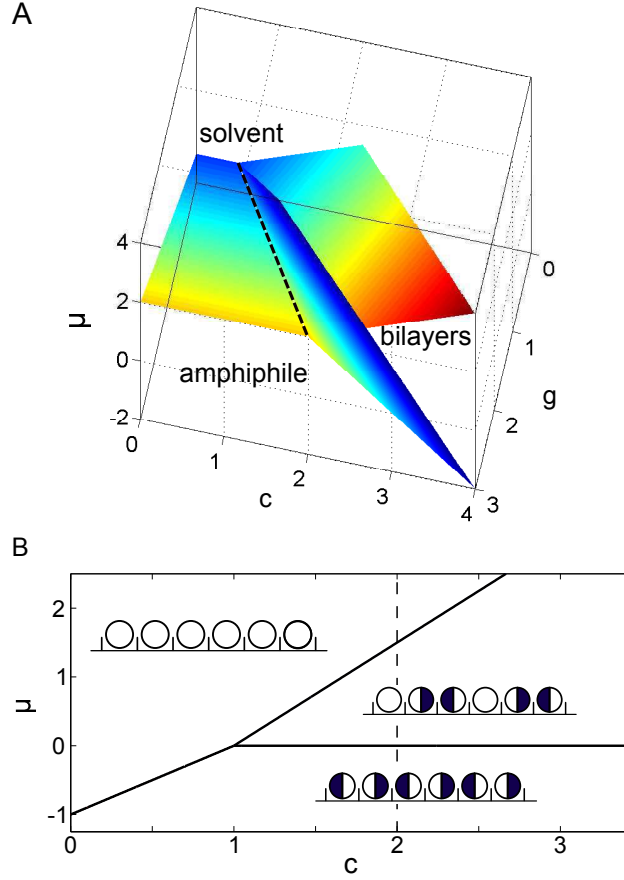


FIG. 2: The ground state of the model in the variables  $(c, g, \mu)$  (panel A) and in the plane  $(c, \mu)$  for  $c = g$  (panel B). The surfaces in panel A represent coexistence between the phases, while the black dashed line represents the triple points where all the three phases coexist. The triple point for  $g = c$  is at  $(c, \mu) = (1, 0)$ . On the B panel a schematic illustration of the three phases is shown in the insets inside the region of stability of each phase. At the coexistence with the solvent-rich phase the layers of solvent,  $l$ , can have an arbitrary length, and at the coexistence with the amphiphile-rich phase the layers of amphiphilic molecules can have the thickness  $2n$  with arbitrary  $n$ . The dashed line corresponds to  $c = g = 2$  for which the EOS, the correlation function and the specific heat are calculated in the following sections.

### III. EXACT EXPRESSIONS FOR PRESSURE, DENSITY AND THE CORRELATION FUNCTION IN TERMS OF THE TRANSFER MATRIX

In this section we introduce the transfer matrix and develop exact expressions for the grand thermodynamic potential, the average density of each component and for the correlation function. The elements of the transfer matrix  $\mathbf{T}$  are given by

$$\mathbf{T}_{ij} \equiv \exp \left\{ -\beta^* \left( V_{ij} - \mu \delta_{i1}^{Kr} \right) \right\}, \quad (5)$$

where  $\delta_{i1}^{Kr}$  is 1 for  $i = 1$  and 0 otherwise, and  $\beta^* = 1/T^* = b/(k_B T)$  with  $k_B$  denoting the Boltzmann constant. The partition function for a system with periodic boundary conditions is

$$\Xi = \sum_{\hat{\rho}(1)} \dots \sum_{\hat{\rho}(L)} \prod_{n=1}^L \exp \left\{ -\beta^* \left[ \hat{\rho}^T(n) \mathbf{V} \hat{\rho}(n+1) - \mu \hat{\rho}_1(n) \right] \right\}. \quad (6)$$

where  $\hat{\rho}(x)^T = (\hat{\rho}_1(x), \hat{\rho}_2(x), \hat{\rho}_3(x))$  denotes the microscopic state at the site  $x$ , and is transverse to the columnar vector  $\hat{\rho}(x)$ . At each lattice site there can be one of the 3 microscopic states  $(1, 0, 0)$ ,  $(0, 1, 0)$ , or  $(0, 0, 1)$ . In terms of the transfer matrix  $\Xi$  takes the form

$$\Xi = \text{Tr} \mathbf{T}^L = \lambda_1^L + \lambda_2^L + \lambda_3^L, \quad (7)$$

where  $\lambda_i$  is the eigenvalue of the transfer matrix. If we denote  $\lambda_1 = \max_{i \in \{1,2,3\}} (|\lambda_i|)$ , the partition function for the system size  $L \gg 1$  takes the even simpler asymptotic form

$$\Xi \simeq \lambda_1^L. \quad (8)$$

In the thermodynamic limit the grand potential in  $b$  units,  $\Omega^* = \Omega/b$ , is given by the exact formula

$$\lim_{L \rightarrow \infty} \Omega^*/L = -p^* = -T^* \lim_{L \rightarrow \infty} \frac{\ln \Xi}{L} = -T^* \ln \lambda_1, \quad (9)$$

where  $p^*$  is 1 dim. pressure in  $b/a$  units.

The average density of the  $i$ -th state is independent of  $x$  because of the translational invariance, and is given by

$$\langle \hat{\rho}_i(1) \rangle = \frac{1}{\Xi} \sum_{\hat{\rho}(1)} \dots \sum_{\hat{\rho}(L)} \prod_{n=1}^L \hat{\rho}_i(1) \exp \left\{ -\beta^* \left[ \hat{\rho}^T(n) \mathbf{V} \hat{\rho}(n+1) - \mu \hat{\rho}_1(n) \right] \right\}. \quad (10)$$

If we change the basis of  $\mathbf{T}$  with a help of the invertible matrix  $\mathbf{P}$  such that  $\mathbf{P}^{-1} \mathbf{T} \mathbf{P}$  is diagonal, then the average density in thermodynamic limit is given by the following expression:

$$\langle \hat{\rho}_i \rangle = \langle \hat{\rho}_i(1) \rangle = \lim_{L \rightarrow \infty} \frac{1}{\Xi} \mathbf{P}_{1i}^{-1} \lambda_1^L \mathbf{P}_{i1} = \mathbf{P}_{1i}^{-1} \mathbf{P}_{i1}. \quad (11)$$

The correlation function  $G_{ii}(n)$  between two sites in the same state  $i$  separated by  $n$  sites is given by

$$G_{ii}(n) = \langle \hat{\rho}_i(1)\hat{\rho}_i(n+1) \rangle - \langle \hat{\rho}_i(1) \rangle \langle \hat{\rho}_i(n+1) \rangle, \quad (12)$$

where

$$\langle \hat{\rho}_i(1)\hat{\rho}_i(n+1) \rangle = \frac{1}{\Xi} \mathbf{T}^n [\hat{\rho}_i(1), \hat{\rho}_i(n+1)] \mathbf{T}^{L-n} [\hat{\rho}_i(n+1) \hat{\rho}_i(1)]. \quad (13)$$

We change the basis to the one in which  $\mathbf{T}$  is diagonal, take the thermodynamic limit and obtain the exact formula,

$$\begin{aligned} \langle \hat{\rho}_i(1)\hat{\rho}_i(n+1) \rangle &= \sum_{k=1}^3 \left( \frac{\lambda_k}{\lambda_1} \right)^n \mathbf{P}_{ik} \mathbf{P}_{ki}^{-1} \mathbf{P}_{i1} \mathbf{P}_{1i}^{-1} \\ &= \langle \hat{\rho}_i \rangle^2 + \sum_{k=2}^3 \left( \frac{\lambda_k}{\lambda_1} \right)^n A_i^{(k)} B_i^{(k)}, \end{aligned} \quad (14)$$

where

$$A_i^{(k)} = \mathbf{P}_{ik} \mathbf{P}_{1i}^{-1}, \quad B_i^{(k)} = \mathbf{P}_{ki}^{-1} \mathbf{P}_{i1} \quad (15)$$

From (14) and (12) we obtain the correlation function

$$G_{ii}(n) = \sum_{k=2}^3 \left( \frac{\lambda_k}{\lambda_1} \right)^n A_i^{(k)} B_i^{(k)}. \quad (16)$$

Eq. (16) can be further simplified for  $n \gg 1$ . In such a case we can neglect the smallest components of the sum in Eq.(16). If the second largest (in the absolute value) eigenvalue  $\lambda_2$  is a pure real number, then  $G_{ii}(n) = \left( \frac{\lambda_2}{\lambda_1} \right)^n A_i^{(2)} B_i^{(2)}$ , but if the  $\lambda_2$  has a non-zero imaginary part, then we have to take into account also the eigenvalue  $\lambda_3$ , complex conjugate to  $\lambda_2$ . Let us introduce the notations

$$\lambda_2 = Z_\lambda e^{\lambda i} \quad A_1^{(2)} = Z_\alpha e^{\alpha i} \quad B_1^{(2)} = Z_\gamma e^{\gamma i} \quad (17)$$

and

$$\xi = \left( \ln \left( \frac{\lambda_1}{Z_\lambda} \right) \right)^{-1}. \quad (18)$$

In terms of these parameters the correlation function for large separations between the particles in an infinite system takes the asymptotic form

$$G_{11}(n) \stackrel{n \gg 1}{\simeq} 2Z_\alpha Z_\gamma e^{-n/\xi} \cos(n\lambda + \alpha + \gamma). \quad (19)$$

#### IV. EQUATION OF STATE

We choose stronger interactions between the amphiphilic than between the solvent molecules,  $c = g = 2$ . For such interaction parameters the periodic phase is present on the GS (see the dashed line in Fig.2B). In Fig.3 we show the concentration  $\rho_s$  (average density of the amphiphile) as a function of the reduced chemical potential difference  $\mu$ . Note the rounded steps for  $\mu \approx 0$  and  $\mu \approx 1.5$ . The steps occur for the values of  $\mu$  corresponding to the GS phase transitions between the periodic and the amphiphile-rich or solvent-rich phases respectively. Between the steps the plateaus for the three densities,  $\rho_s = 1, 2/3, 0$  occur. For increasing  $T^*$  the  $\rho_s(\mu)$  lines become smoother, but the inflection points exist up to  $T^* \approx 0.2$ .

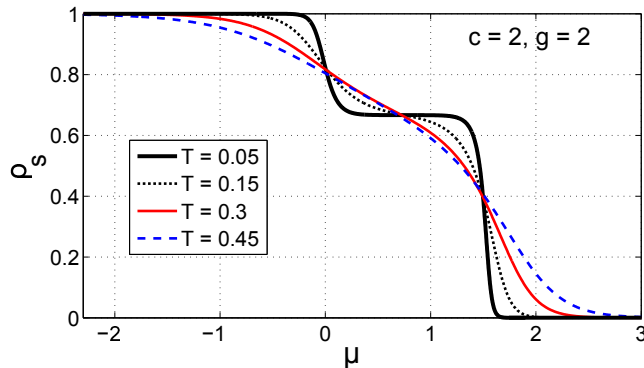


FIG. 3: Average density of the amphiphile,  $\rho_s = 1 - \rho_1 = \rho_2 + \rho_3$ , for  $c = g = 2$  at  $T^* = 0.05, 0.15, 0.3, 0.45$  as a function of the reduced chemical potential difference  $\mu$ .

In Eqs.(9) and (11) the pressure and the average density are expressed in terms of  $T^*$  and the reduced chemical potential difference  $\mu$ . By eliminating  $\mu$  we can obtain the dependence of the amphiphile density on  $p^*$ . We present  $\rho_s(p^*)$  in Fig.4. Note that although there are no phase transitions in the strict sense in 1d, for low  $T^*$  there is a rapid change in  $\rho_s$  between  $\rho_s = 1$  and  $\rho_s = 2/3$  for a very small  $p^*$  interval near  $p^* \approx 2$ , almost constant amphiphile density between  $p^* \approx 2$  and  $p^* \approx 2.5$ , and again a rapid change of  $\rho_s$  between  $2/3$  and nearly 0 for  $p^* \approx 2.5$ . This behavior suggests the pseudo-phase transitions between the amphiphile-rich and the periodic pseudo-phase with the density  $\rho_s \approx 2/3$  (see Fig.2b) and next between the periodic pseudo-phase and the solvent-rich pseudo-phase. For increasing temperature the changes of the slope of the  $\rho_s(p^*)$  line for increasing  $p^*$  become smaller. This result should be contrasted with the pressure-concentration dependence shown in Fig.5

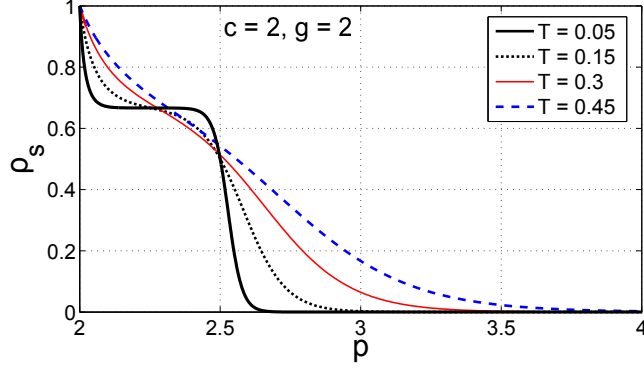


FIG. 4: Average density of the amphiphile,  $\rho_s = 1 - \rho_1 = \rho_2 + \rho_3$ , for  $c = g = 2$  at  $T^* = 0.05, 0.15, 0.3, 0.45$ . As the energy unit we choose the interaction  $b$  between the two solvent molecules, and the length unit is the lattice constant  $a$ . We assume that  $a$  is of order of the size of the amphiphilic molecules. In the case of lipids  $a \sim 2nm$ .

for the interaction parameters such that the periodic phase is not stable at the GS.

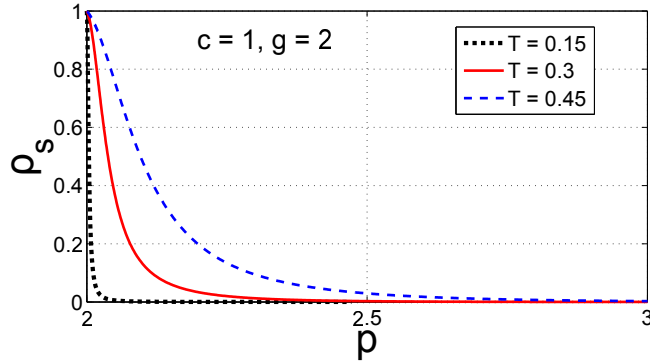


FIG. 5: Average density of the amphiphile,  $\rho_s = 1 - \rho_1 = \rho_2 + \rho_3$ , for  $c = 1$   $g = 2$  and  $T^* = 0.15, 0.3, 0.45$ . As the energy unit we choose the interaction  $b$  between the two solvent molecules, and the length unit is the lattice constant  $a$ . We assume that  $a$  is of order of the size of the amphiphilic molecules. In the case of lipids  $a \sim 2nm$ .

## V. CORRELATION FUNCTION

In the case of the periodic boundary conditions the system is translationally invariant, and the assembly into bilayers should be reflected in the shape of the correlation function. When the bilayers are formed, then the correlation function for the solvent,  $G_{11}(x)$  should be

negative for two subsequent values of  $x$ , where the properly oriented amphiphilic molecules should appear with larger probability than the solvent molecule. The exact results for  $G_{11}(x)$ , given in Eq.(16), are shown in Fig.6 for  $\mu = 1$ , i.e. for the GS stability of the periodic phase, for a few rather high temperatures. We can see the oscillatory decay of correlations, with the period 3 as in the case of the concentration in the GS periodic phase. The decay length decreases with increasing temperature. Only for short distances  $G_{11}(x) < 0$  for two subsequent values of  $x$ , however.

In Figs.7 and 8 we show  $G_{11}(x)$  for very low  $T^*$  and a few values of  $\mu$  close to the GS coexistence between the periodic and the solvent- or amphiphile-rich phases. Very large correlation length, 3 orders of magnitude larger than the molecular size, can be seen inside the GS stability of the periodic phase.

The correlation length  $\xi$  (see Eq.(18)) and the period of the damped oscillatory decay (see Eq.(19)) are shown in Fig.9. We can see that  $\xi \rightarrow 0$  beyond the GS stability of the periodic phase, i.e. for  $\mu < 0$  and  $\mu > 1.5$ . Moreover, for  $0 < \mu < 1.5$  the period of the damped oscillations is  $2\pi/\lambda \approx 3$ .

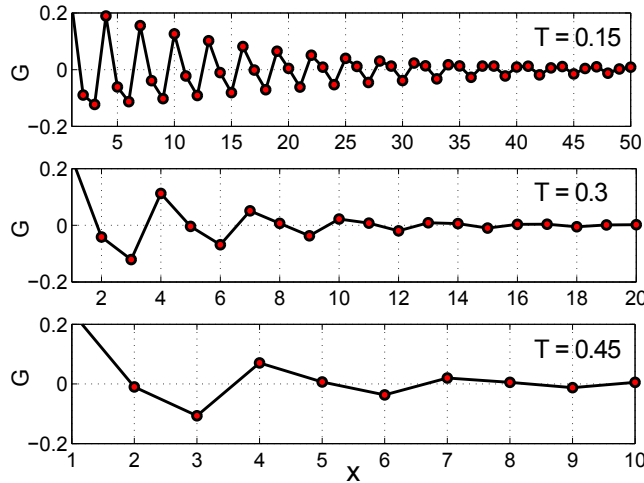


FIG. 6: Correlation function between the solvent molecules at  $T = 0.15, 0.3, 0.45$  for  $g = c = 2$  and  $\mu = 1$ .

Let us focus on the structure for the interaction parameters corresponding to the absence of the periodically distributed bilayers in the GS. We choose  $c = 0.623$  and  $g = 0.25$ . The correlation length  $\xi$  and the period  $2\pi/\lambda$  of the damped oscillatory decay for  $c = 0.623$  and  $g = 0.25$ , and different temperatures are shown in Fig.10. For  $T^* \leq 0.2$  the eigenvalue  $\lambda_2$

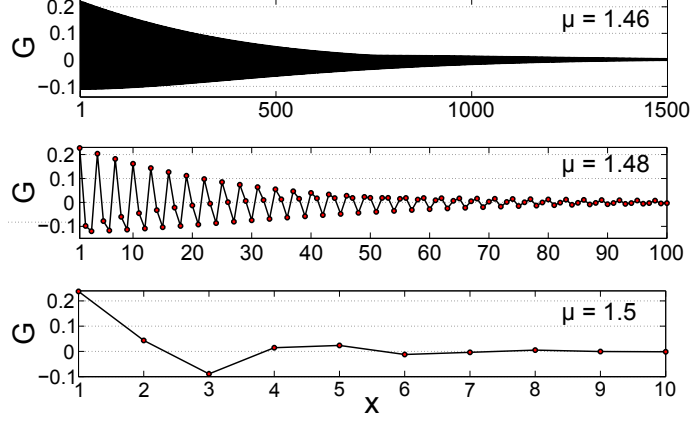


FIG. 7: Correlation function between the solvent molecules at  $T = 0.005$  for  $g = c = 2$  and  $\mu = 1.46$  (a),  $\mu = 1.48$  (b),  $\mu = 1.5$  (c), with  $\mu = 1.5$  being the value of the chemical potential at the coexistence between the periodic and the solvent-rich phases at the GS.

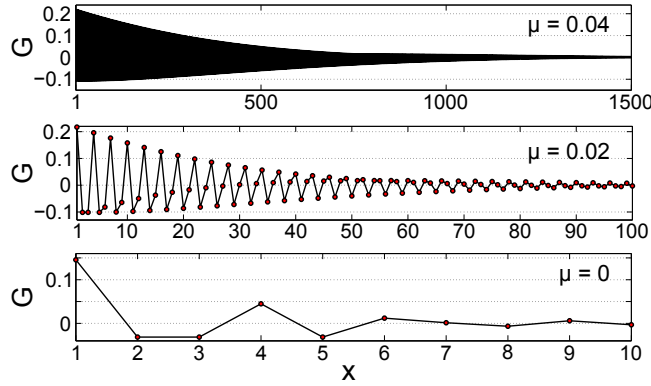


FIG. 8: Correlation function between the solvent molecules at  $T = 0.005$  for  $g = c = 2$  and  $\mu = 0.04$  (a),  $\mu = 0.02$  (b),  $\mu = 0$  (c), with  $\mu = 0$  being the value of the chemical potential at the coexistence between the periodic and the amphiphile-rich phases at the GS.

is a pure real number for any value of the chemical potential, and the correlation function decays monotonically. The change of the  $\xi$  slope around  $\mu = -0.39$  at  $T^* = 0.2$  indicates the point where  $\lambda_2$  changes sign. The period of the oscillatory decay jumps from zero to infinity at this point. Both cases correspond to the monotonic decay of correlations, but at this point ( $\mu = -0.39$  and  $T^* = 0.2$ ) an oscillatory decay for  $T^* > 0.2$  and a range of  $\mu$  around  $\mu = -0.39$  begins. This is because for  $T^* > 0.2$  there are two discontinuities of the derivative of  $\xi$  (e.g. at  $\mu_1$  and  $\mu_2$  for  $T^* = 0.3$ ). Between the two points of discontinuity of  $\partial\xi/\partial\mu$ , the  $\lambda_2$  is a complex number, and hence for this interval of  $\mu$  the correlation function

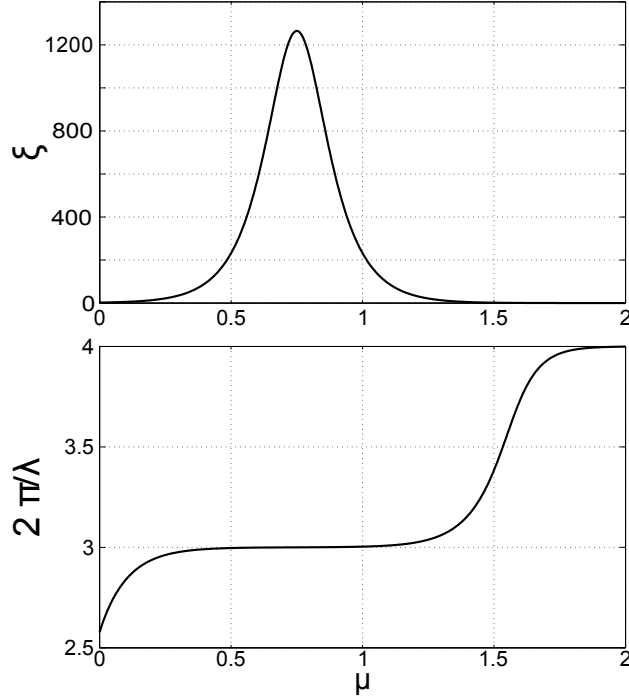


FIG. 9: The correlation length  $\xi$  and the period of the oscillatory decay of correlations (Eqs.(18) and (19)) for  $g = c = 2$  and  $T = 0.1$ . For  $\mu = 0$  and  $\mu = 1.5$  the periodic phase coexists with the amphiphile and the solvent respectively at  $T = 0$ .

has an oscillatory decay. Note that for  $c = 0.623, g = 0.25$  the periodic phase is not stable on the GS, and counterintuitively the oscillatory decay of  $G_{11}(x)$  occurs at higher  $T^*$ . However, the correlation length is smaller than the period of the damped oscillations. Similar change from the monotonic to the oscillatory decay of correlations for increasing temperature has been obtained for the SALR system in Ref.[24].

## VI. SPECIFIC HEAT

In this section we consider the specific heat for a fixed concentration. Fixed concentration imposes a global constraint on the microstates, therefore exact analytical calculations directly in the canonical ensemble are less easy. To overcome this difficulty, we first calculate the specific heat for fixed chemical potential using the exact results of sec.3. In order to compute the specific heat for fixed concentration we use the thermodynamic relations. For comparison we perform Monte Carlo (MC) simulations in the canonical ensemble.

The specific heat of a mixture with fixed number of all particles and fixed chemical

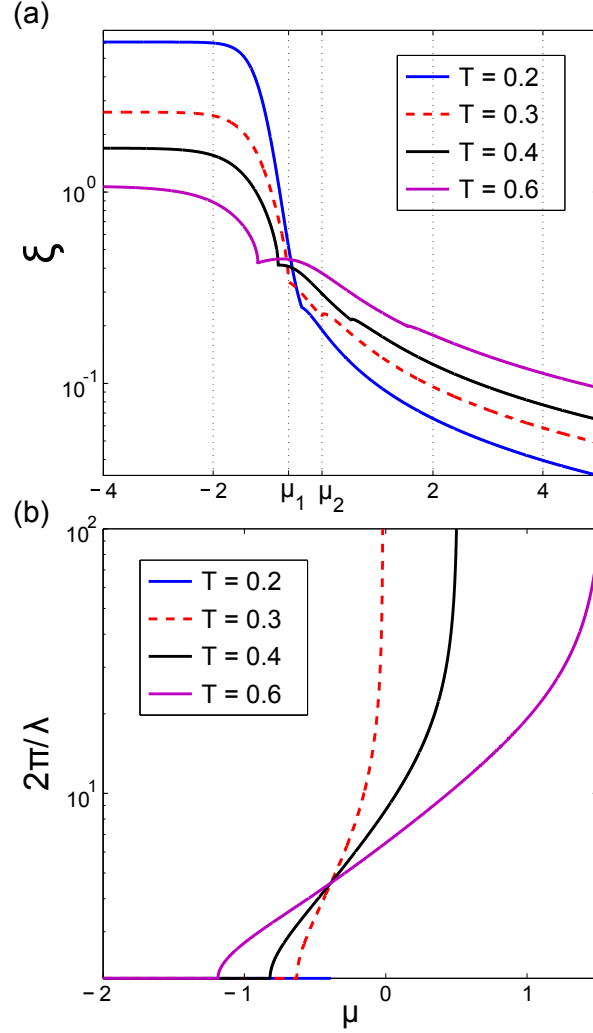


FIG. 10: The correlation length  $\xi$  and the period of the oscillatory decay of correlations for  $c = 0.623, g = 0.25$  at  $T^* = 0.2, 0.3, 0.4, 0.6$ . For  $\mu = -0.75$  the amphiphile and the solvent coexist at  $T^* = 0$ . For  $T^* < 0.2$  the monotonic decay of correlations between the solvent molecules is obtained. At  $T^* = 0.2$  the period of the oscillatory decay jumps from zero to infinity for  $\mu \approx -0.39$ . For  $T^* > 0.2$  the correlation function for the solvent exhibits an oscillatory decay for some range of  $\mu$ . In the case of  $T^* = 0.3$  the oscillatory decay occurs for  $\mu_1 < \mu < \mu_2$ . Note the logarithmic scale on the vertical axis.

potential difference between the components,  $\mu$ , is given by

$$c_\mu = -\frac{T}{L} \left( \frac{\partial^2 \Omega^*}{\partial T^2} \right)_{\mu, V} \quad (20)$$

where the exact expression for  $\Omega^*$  is given in Eq.(9). We compute  $c_v$  using the following

relations,

$$c_v = c_\mu - T \left( \frac{\partial \rho_\mu}{\partial T} \right)^2 \left( \frac{\partial \rho_\mu}{\partial \mu} \right)^{-1} \quad (21)$$

and

$$\rho_\mu(T, \mu) = -\frac{1}{L} \left( \frac{\partial \Omega^*}{\partial \mu} \right)_{T,V}. \quad (22)$$

In order to verify the exact calculations based on the grand canonical ensemble, we performed MC simulations in the canonical ensemble with the sampling procedure based on the Metropolis algorithm [35]. The sampling is made with two kind of MC steps: (i) the exchange of lipid and water molecules positions (ii) the change of lipid molecule orientation. The specific heat per lattice site is computed using the fluctuation formula:

$$c_v = \frac{1}{Lk_B T^2} [\langle H^2 \rangle - \langle H \rangle^2] \quad (23)$$

where here  $\langle \dots \rangle$  is the average over the microstates in the canonical ensemble. The simulations were performed for  $L \leq 4800$ . We verified that the finite size effects are negligible for  $L = 4800$  (see Fig.11a).

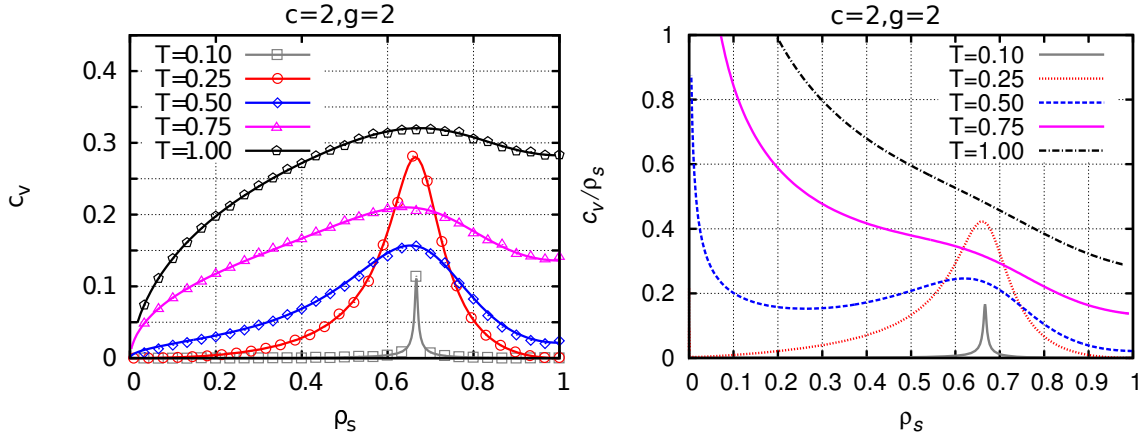


FIG. 11: The specific heat for fixed concentration  $\rho_s$  as a function of  $\rho_s$  for  $c = g = 2$  and different temperatures. Top: per unit volume ( $c_v$ ). Bottom: per amphiphilic molecule ( $c_v/\rho_s$ ). Symbols denote the results of the Monte Carlo simulations for  $L = 4800$ , and lines represent the analytical results in thermodynamic limit (Eqs. (20)- (22) and (9)).

In order to compare thermal properties of this model and the SALR model of Ref.[24], we should note that in the case of the colloidal self-assembly the specific heat was calculated per colloid particle, and the solvent was disregarded. The specific heat per unit volume

calculated here is a different quantity, therefore in Fig.11b we present  $c_v/\rho_s$  representing the specific heat per amphiphilic molecule. Note that in this model the specific heat of the pure solvent (i.e. for  $\rho_s = 0$ ) vanishes, since the energy does not fluctuate when all the sites are occupied by the solvent. In this respect the solvent is analogous to the disregarded solvent in the SALR model. Thus, to compare the thermal effects of the amphiphilic and the colloidal self-assembly, we shall compare  $c_v/\rho_s$  obtained here and the specific heat per colloid particle calculated in Ref.[24].

Let us first discuss the specific heat for  $c = g = 2$ . For such interactions three phases are present on the GS: the solvent-rich for  $\rho_s = 0$ , the periodic array of bilayers for  $\rho_s = 2/3$  and the amphiphile-rich for  $\rho_s = 1$ . The formation of the periodic phase at  $T^* = 0$  is indicated by the peak for  $\rho_s = 2/3$  that becomes narrower for decreasing temperature (Fig.11a). In Fig. 11b an increase of  $c_v/\rho_s$  for  $\rho_s \rightarrow 0$  can be observed for the range of  $\rho_s$  that increases with increasing  $T^*$ . This behaviour may be associated with an equilibrium between bilayers and isolated amphiphilic molecules. In the SALR system the qualitative behavior of the specific heat is similar. The peak for the density corresponding to the stability of the periodic phase that becomes narrower for decreasing temperature, and another maximum for a very small density are both present [24].

For  $c = 1, g = 2$  only the solvent-rich and the amphiphile-rich phases are stable at the GS. The absence of the periodic phase leads to a lack of the peak in the specific heat for  $\rho_s = 2/3$ . As in the previous case an increase of  $c_v/\rho_s$  for  $\rho_s \rightarrow 0$  can be observed. The  $c_v/\rho_s$  in this case is also similar to the specific heat in the SALR system for the interactions such that only the two homogeneous phases are present on the GS [24].

Note that from Figs.11 and 12 it follows that the dependence of  $c_v$  on  $T$  for fixed  $\rho_s$  is nontrivial, and differs qualitatively from  $c_v(T)$  in the lattice gas or Ising model. In the latter models a single maximum of  $c_v(T)$  occurs, whereas in this model two maxima separated by a minimum are present. The simulation snapshots indicate formation of solvent-separated bilayers at low  $T^*$  for  $\rho_s \leq 1/3$ . Between the two maxima of  $c_v(T)$  amphiphiles, oriented head-to-head or tail-to-tail, form larger domains separated by domains of solvent. At the second maximum random positions and orientations of the amphiphiles appear. The two maxima of  $c_v(T)$  are present even for  $c, g$  such that only the pure solvent and pure amphiphiles are present at the GS. In such a case phase-separated solvent and amphiphiles, or random positions and orientations are present for low  $T^*$  or for high  $T^*$  respectively, whereas

between the two maxima of  $c_v(T)$  domains of solvent and properly oriented amphiphiles are formed.

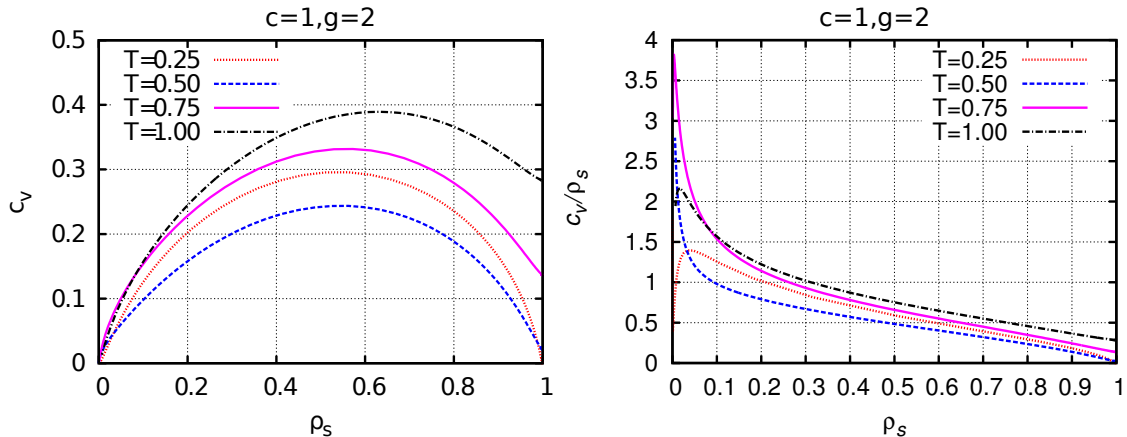


FIG. 12: The specific heat for fixed concentration  $\rho_s$  as a function of  $\rho_s$  for  $c = 1$  and  $g = 2$  and different temperatures. Left: per unit volume ( $c_v$ ). Right: per amphiphilic molecule ( $c_v/\rho_s$ ). Lines represent the analytical results in thermodynamic limit (Eqs. (20)- (22) and (9)).

## VII. COMPARISON BETWEEN THE AMPHIPHILIC AND COLLOIDAL SELF-ASSEMBLY AND CONCLUDING REMARKS

We have solved exactly the simple lattice model for amphiphilic mixtures introduced in Ref.[25]. The ground-state shows that the model predicts the key properties of aqueous solutions of amphiphilic molecules such as lipids. It also helps to understand the relation between the degeneracy of the ground state and the low surface tension.

For  $T^* > 0$  we have obtained oscillatory decay of correlations for the range of  $\mu$  corresponding to the GS stability of the periodic phase. The oscillatory decay of correlations indicates alternating layers of the solvent and the properly oriented amphiphilic molecules. For small  $T^*$  and for the range of the chemical potential  $\mu$  corresponding to the GS stability of the periodic phase the correlation length is very large, a few orders of magnitude larger than the molecular size. Thus, the correlation function is consistent with a quasi long-range order.

The periodic ordering at low temperatures is reflected in the shape of the  $\rho_s(p^*)$  line too. The average density  $\rho_s \approx 2/3$  is nearly independent of pressure for a large pressure interval.

These two results are consistent with a formation of solvent-separated bilayers in domains of a size of order of micrometers. For increasing  $T^*$  the correlation length decreases, and the line  $\rho_s(p^*)$  becomes smoother. Finally, the specific heat assumes a maximum for the concentration of amphiphiles  $\rho_s = 2/3$  corresponding to the GS stability of the periodic phase. The maximum becomes very narrow for low  $T^*$ . When the periodic phase is not present on the GS (see Fig.2), the maximum of the specific heat per amphiphilic molecule for  $\rho_s = 2/3$  is absent.

We have found strong similarity of the  $T = 0$  phase diagrams for the present model for amphiphilic self-assembly (Fig.2) and for the lattice model for colloidal self-assembly (Fig.1 in Ref. [24]). The phases with oscillatory density in the SALR systems or oscillatory concentration in the amphiphilic mixtures occur when the repulsion in the case of the colloids or attraction between the solvent and properly oriented amphiphilic molecules are sufficiently strong. When the above interactions are weak, only two phases are present in the ground state, namely the gas and liquid in the SALR case, and the pure water and amphiphile phases in the present model.

It is interesting that the ground state has the same kind of degeneracy at the phase coexistence between the periodic phase and the pure solvent for both, the amphiphilic and the colloidal self-assembly [24, 36]. In both models the ground state is strongly degenerate, and the surface tension between the homogeneous and the periodic phase vanishes for  $T = 0$ , although in the case of the colloidal self-assembly the particles have neither shape nor interaction anisotropy. Arbitrary number of arbitrarily small droplets of the coexisting phases can be present at the phase coexistence. This degeneracy of the ground state means that the macroscopic separation of the two phases at  $T \rightarrow 0$  is not possible, since the formation of an interface does not lead to any increase of the grand potential. At the same time, because of the microscopic size of the droplets, one can interpret the degenerate ground state as a disordered phase. The region of the  $T = 0$  phase diagram corresponding to the stability of this phase is of zero measure, however, in contrast to the remaining, ordinary phases. Note that the ultra-low surface tension is a generic property of systems with competing tendencies in the interactions that lead to stability of periodic structures, and is not limited to amphiphilic molecules.

The exact results for the present model and for the model of colloidal self-assembly show that the low surface tension is a more general property of systems with competing

interactions, and is not limited to amphiphilic molecules. This confirms the observation of universality of the periodic ordering on the mesoscopic length scale that was derived under the assumption of weak ordering [20].

The effect of the inhomogeneous density or concentration in the above systems on the equation of state has been studied in the framework of the statistical thermodynamics only very recently [24, 37]. We have found strong similarity between the pressure-density isotherm in the SALR system [24] and the pressure-concentration isotherm in our model of the amphiphilic mixture. The characteristic feature of these lines is the plateau in the density or concentration as a function of pressure. Similar shapes have also the density - chemical potential and the concentration - chemical potential lines. The plateau occurs when the density or concentration takes the value corresponding to the periodic distribution of the clusters or the bilayers. For the corresponding range of  $\mu$  and  $T^*$  the correlation functions in both models exhibit exponentially damped oscillatory decay with a very large correlation length. The thermal properties are also similar. In both models the specific heat assumes a maximum for the density or concentration corresponding to the GS periodic phase. In addition, the specific heat per particle in the SALR case or per amphiphilic molecule in this model increase for decreasing number of particles or amphiphilic molecules. This behavior is associated with the equilibrium between the clusters and isolated particles or between the bilayers (or micelles) and isolated amphiphiles.

The main difference between the self-assembly in the amphiphilic and colloidal systems concerns the periodic ordering of the pure amphiphiles into the lamellar structure that is absent in the dense phase in the colloidal system.

To conclude, the exact results in the present model for amphiphilic systems and in the lattice model for the SALR systems [24] demonstrate close similarity between different types of self-assembly.

### **Acknowledgments**

This work is dedicated to Prof. Tomas Boublik and Prof. Ivo Nezbeda. A part of this work was realized within the International PhD Projects Programme of the Foundation for Polish Science, cofinanced from European Regional Development Fund within Innovative Economy Operational Programme "Grants for innovation". AC and PR acknowledge the financial support by the National Science Center grant 2012/05/B/ST3/03302. JP acknowledges the financial support by the National Science Center under Contract Decision No.

- [1] T. Boublik, K. Hlavaty, and I. Nezbeda, *Statistical thermodynamics of simple liquids and their mixtures* (Amsterdam: Elsevier, 1980).
- [2] J. Kolafa and I. Nezbeda, *Fluid Phase Equil.* **100**, 1 (1994).
- [3] V. D. Nguyen, S. Faber, Z. Hu, G. H. Wegdam, and P. Schall, *Nature communications* **4**, 1584 (2013).
- [4] A. Stradner, H. Sedgwick, F. Cardinaux, W. Poon, S. Egelhaaf, and P. Schurtenberger, *Nature* **432**, 492 (2004).
- [5] A. I. Campbell, V. J. Anderson, J. S. van Duijneveldt, and P. Bartlett, *Phys. Rev. Lett.* **94**, 208301 (2005).
- [6] M. Teubner and R. Strey, *J. Chem. Phys.* **87**, 3195 (1987).
- [7] M. K. Kahlweit, R. Strey, and P. Firman, *J. Phys. Chem.* **90**, 671 (1986).
- [8] G. Gompper and M. Schick, *Self-Assembling Amphiphilic Systems*, vol. 16 of *Phase Transitions and Critical Phenomena* (Academic Press, London, 1994), 1st ed.
- [9] A. Ciach and W. T. Gózdź, *Annu. Rep. Prog. Chem., Sect. C: Phys. Chem* **97**, 269-314 (2001), and references therein.
- [10] A. J. Archer, D. Pini, R. Evans, and L. Reatto, *J. Chem. Phys.* **126**, 014104 (2007).
- [11] A. J. Archer and N. B. Wilding, *Phys. Rev. E* **76**, 031501 (2007).
- [12] R. P. Sear and W. M. Gelbart, *J. Chem. Phys.* **110**, 4582 (1999).
- [13] D. Pini, A. Parola, and L. Reatto, *J. Phys.:Cond. Mat.* **18**, S2305 (2006).
- [14] A. Ciach and W. T. Gózdź, *Condensed Matter Physics* **13**, 23603 (2010).
- [15] A. de Candia, E. Del Gado, A. Fierro, N. Sator, M. Tarzia, and A. Coniglio, *Phys. Rev. E* **74**, 010403(R) (2006).
- [16] J. Toledano, F. Sciortino, and E. Zaccarelli, *Soft Matter* **5**, 2390 (2009).
- [17] A. J. Archer, *Phys. Rev. E* **78**, 031402 (2008).
- [18] L. Latypova, W. T. Gozdz, and P. Pieranski, *Eur. Phys. J. E* **36**, 88 (2013).
- [19] M.W.Matsen and M. Schick, *Curr. Op. Colloid and Interf. Sci.* **1**, 329 (1996).
- [20] A. Ciach, J. Pękaliski, and W. T. Gózdź, *Soft Matter* **9**, 6301 (2013).
- [21] S. A. Brazovskii, *Sov. Phys. JETP* **41**, 85 (1975).

- [22] L. Leibler, *Macromolecules* **13**, 1602 (1980).
- [23] W. T. Gózdź and R. Hołyst, *Phys. Rev. E* **54**, 5012 (1996).
- [24] J. Pękałski, A. Ciach, and N. G. Almarza, *J. Chem. Phys.* **138**, 144903 (2013).
- [25] A. Ciach and J. Pękałski, arXiv:1407.0816 [cond-mat.soft] (2014).
- [26] A. Imperio and L. Reatto, *J. Chem. Phys.* **124**, 164712 (2006).
- [27] A. Ciach, J. S. Høye, and G. Stell, *J Phys A* **21**, L777 (1988).
- [28] A. Ciach and M. Tasinkevych, *Mol. Phys.* **109**, 2907 (2011).
- [29] I. Brovchenko and A. Oleinikova, *Chem. Phys. Chem* **9**, 2660 (2008).
- [30] J. Jirsak and I. Nezbeda, *J. Mol. Liq.* **136**, 310 (2007).
- [31] I. Nezbeda and J. Jirsak, *Phys. Chem. Chem. Phys.* **13**, 19689 (2011).
- [32] A. Ciach, W. T. Gózdź, and A. Perera, *Phys. Rev. E* **78**, 021203 (2008).
- [33] A. Perera and B. Kezic, *Faraday Discuss.* **167**, 145 (2013).
- [34] J. Kolafa and I. Nezbeda, *Mol. Phys.* **61**, 161 (1987).
- [35] A. Ciach, J. S. Høye, and G. Stell, *J. Chem. Phys.* **90**, 1214 (1989).
- [36] J. Pękałski, A. Ciach, and N. G. Almarza, *J. Chem. Phys.* **140**, 114701 (2014).
- [37] A. Ciach and O. Patsahan, *Condens. Matter Phys.* **15**, 23604 (2012).